Uneven compression levels of Earth's magnetic fields by shocked solar wind

J.-H. Shue,[1] Y.-S. Chen,[1] W.-C. Hsieh,[1] M. Nowada,[1] B. S. Lee,[1] P. Song,[2] C. T. Russell,[3] V. Angelopoulos,[3] K. H. Glassmeier,[4] J. P. McFadden,[5] and D. Larson[5]

Received 28 September 2010; revised 25 November 2010; accepted 20 December 2010; published 5 February 2011.

[1] The magnetopause is the boundary where the reduced solar wind dynamic pressure is equal to the magnetic pressure of the Earth's outer magnetosphere. With hundreds of magnetopause crossings identified from the THEMIS data, we estimate a ratio (f) of the compressed magnetic field just inside the subsolar magnetopause to the purely dipolar magnetic field. Previous theoretical studies reported that the ratio f was nearly independent of the subsolar standoff distance (r_0). Here we report that the ratio f is linearly proportional to r_0 for both northward and southward interplanetary magnetic field (IMF). The proportionality constant for southward IMF is larger than that for northward IMF, implying that the compression level of the magnetic field by inward magnetopause for southward IMF is smaller than that for northward IMF.

Citation: Shue, J.-H., et al. (2011), Uneven compression levels of Earth's magnetic fields by shocked solar wind, *J. Geophys. Res.*, *116*, A02203, doi:10.1029/2010JA016149.

1. Introduction

[2] The internal magnetic field of the Earth would be well approximated as a dipolar field if there were no solar wind. The solar wind dynamic pressure D_p is reduced when the solar wind flows around the magnetosphere. The reduced dynamic pressure is equal to the magnetic pressure of the Earth's magnetosphere at the subsolar magnetopause, as follows:

$$kD_p = \frac{B_{g0}^2}{2\mu_0}, \tag{1}$$

where k is the reduction factor of the solar wind dynamic pressure, B_{g0} is the compressed magnetic field just inside the subsolar magnetopause, and μ_0 is the permeability in free space. With the assumptions that k is constant and B_{g0} is proportional to r_0^{-3}, the subsolar standoff distance r_0 in terms of D_p can be calculated from (1). However, the two assumptions might not be correct. In this study, we intend to test the latter assumption.

[3] The compression level of the magnetic field can be quantified by a ratio of the magnetic field just inside the subsolar magnetopause to the purely dipolar magnetic field (B_{d0}) that would be calculated at that location if the solar wind were absent, namely, $f = B_{g0}/B_{d0}$. Previous theoretical studies in simple magnetosphere [*Ferraro*, 1960; *Mead*, 1964; *Schield*, 1969; *Choe and Beard*, 1974] found that the ratio f was nearly independent of r_0. However, these studies did not include the process of magnetic reconnection in their models. *Aubry et al.* [1970] first reported that the magnetopause moves inward when magnetic reconnection occurs for southward interplanetary magnetic field (IMF).

[4] Although *Sibeck et al.* [1991] and *Holzer and Slavin* [1978] determined f^2/k from (1) with given observed D_p and r_0, the individual value of f has never been directly determined from observations. Here we determine the ratio f for both southward and northward IMF directly from in situ data from Time History of Events and their Macroscopic Interactions during Substorms (THEMIS). Also, no empirical function of B_{g0} in terms of r_0 has been reported in the literature. Here we derive such empirical functions for both southward and northward IMF. Derivation of these empirical functions can advance our understanding of interactions between the solar wind and the magnetosphere.

2. Data Processing

[5] The five THEMIS probes carry identical instruments, observing plasma and magnetic fields in the solar wind–magnetosphere system [*Angelopoulos*, 2008; *Auster et al.*, 2008; *McFadden et al.*, 2008]. During the mission in 2007 and 2008, the THEMIS probes crossed the dayside magnetopause thousands of times. *Glassmeier et al.* [2008] demonstrated that the THEMIS data are suitable to study the structure and dynamics of the magnetopause and the pressure balance at the magnetopause. Here we directly calculate B_{g0} using the 3 s magnetic field data from THEMIS, and B_{d0} at

[1]Institute of Space Science, National Central University, Jhongli, Taiwan.
[2]Center for Atmospheric Research, University of Massachusetts Lowell, Lowell, Massachusetts, USA.
[3]Institute of Geophysics and Planetary Physics, University of California, Los Angeles, California, USA.
[4]Institute of Geophysics and Extraterrestrial Physics, Technical University Braunschweig, Braunschweig, Germany.
[5]Space Sciences Laboratory, University of California, Berkeley, California, USA.

0148-0227/11/2010JA016149

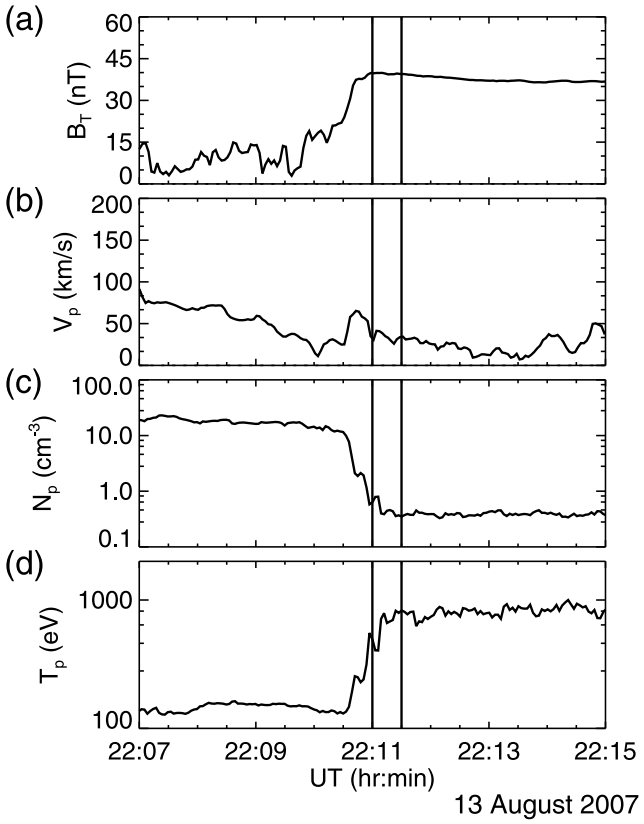

Figure 1. An example of a determination of the average magnetic field just inside the subsolar magnetopause B_{g0}. Around 2210 UT on 13 August 2007, the THEMIS-A probe was located at (12.4, 0.7, 3.4) R_E in the GSM coordinate system, observing (a) the total magnetic field, (b) the speed of ions, (c) the number density of ions, and (d) the average temperature of ions. The magnetopause crossing was identified by the discontinuity of the magnetic field at 2210:30 UT. The interval bounded by the two vertical lines denotes the 30 s period that was used to calculate the average B_{g0}.

the same position from the purely dipolar magnetic field model.

[6] Figure 1 is one of the magnetopause crossings identified from the THEMIS data. Around 2200 UT on 13 August 2007, the THEMIS-A probe was moving inbound near the subsolar magnetopause. The magnetometer on board observed an abrupt increase in the total magnetic field at 2210:30 UT, indicating a high-shear magnetopause crossing [*Paschmann et al.*, 1986]. The magnetic field on the magnetosheath side of the magnetopause was turbulent. A plateau in the magnetic field was found on the magnetospheric side. For some cases, the magnetic field on the magnetospheric side could have transient variations caused by unbalanced pressure. These cases may affect the accuracy of statistics. Therefore, only the magnetopause crossings that had a plateau in the magnetic field were selected for this statistical study. The speed of the solar wind dropped to a very small value as the flow reached the magnetopause. The density of ions dropped suddenly, and the temperature of ions jumped when THEMIS moved inbound. B_{g0} was calculated by averaging the magnetic field data for a 30 s period that was chosen to its visibly close proximity to the magnetopause, as bracketed by the two vertical lines in Figure 1.

[7] Solar wind conditions corresponding to each magnetopause crossing, including D_p and IMF B_z, were obtained by using 1 min plasma and magnetic fields from the NASA OMNI database [*King and Papitashvili*, 2005]. The 1 min OMNI data were shifted for the propagation time from a solar wind monitor to the nose of the bow shock. We averaged the OMNI data over the 6 min period centered at the time of a magnetopause crossing to represent the corresponding solar conditions. The average D_p for all the magnetopause crossings (1.47 nPa) is smaller than the normal value (2.60 nPa, calculated by *Kivelson and Russell* [1995] with the average solar wind velocity 450 km/s and density 6.6 cm^{-3}). Note that the calculation of D_p has included 4% contribution from solar wind Helium.

[8] In addition to the motion of the Earth around the Sun, the non-Sun-Earth-line component of the solar wind velocity can create an aberration in the position of a magnetopause crossing. We removed these aberration effects on r_0 before studying the relation between B_{g0} and r_0. Since (1) is valid only at the subsolar magnetopause, the magnetopause crossings observed only within 30° between the Sun-Earth line and the positional vector of the magnetopause in the equatorial plane are suitable for this study. According to *Spreiter and Briggs* [1962] and *Petrinec and Russell* [1995], dipole tilt angle can affect the position of the magnetopause and the magnetic field just inside the magnetopause. We also imposed another criterion by selecting the magnetopause crossings observed only within 15° from the equator in the sum of the latitude of the magnetopause and the dipole tilt angle. In total, 614 subsolar magnetopause crossings survived the selection criteria, 225 of them for southward IMF ($B_z < -1$ nT), and the others (389) for northward IMF ($B_z > 1$ nT).

3. Fitting Procedure

[9] The relation between B_{g0} and r_0 can be modeled with a power law function:

$$B_{g0} = Cr_0^D, \tag{2}$$

where C and D are the parameters of the function. By taking the logarithm of both sides, we have

$$\ln(B_{g0}) = \ln(C) + D\ln(r_0). \tag{3}$$

[10] The variables B_{g0} and r_0 are first transformed into $\ln(B_{g0})$ and $\ln(r_0)$, and then fit each other using the least squares method to a straight line, as shown in Figure 2a. The fitting of the magnetopause crossings for southward IMF results in $\ln(C) = 8.05 \pm 0.26$ and $D = -1.68 \pm 0.11$, where one standard deviation is defined for the error. With an implementation of propagation of errors [*Bevington and Robinson*, 2003], C is equal to 3120 ± 14 nT. Equation (2) can be rewritten as

$$B_{g0} = 3120r_0^{-1.68}. \tag{4}$$

[11] The F test is a test to evaluate the confidence level of a fit [*Bevington and Robinson*, 2003]. The critical F tabulated

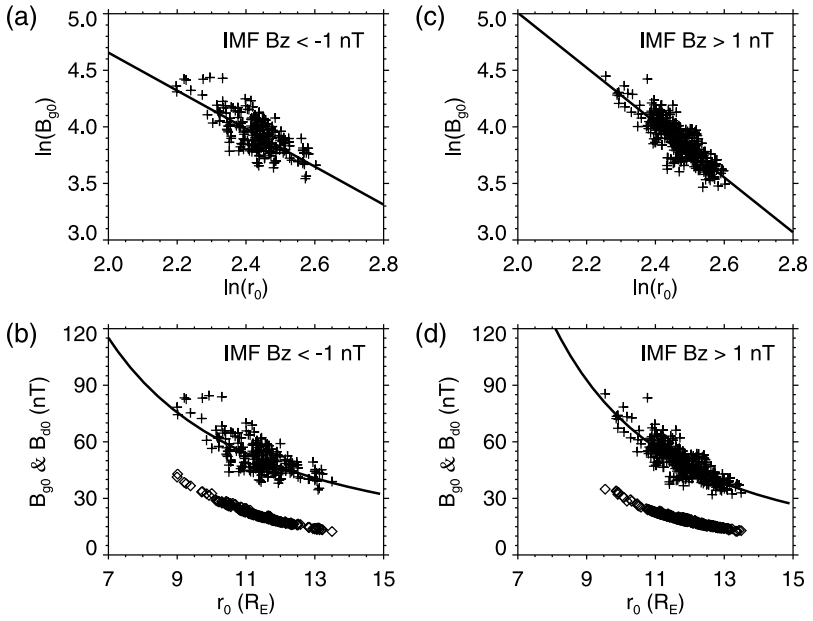

Figure 2. The relation between the compressed magnetic field just inside the subsolar magnetopause B_{g0} and the subsolar distance r_0 for southward IMF and northward IMF. The dipolar magnetic field B_{d0} was calculated at the same position where B_{g0} was observed. The linear least squares method was used to derive the relation. (a) Here $\ln(B_{g0})$ was plotted against $\ln(r_0)$ for southward IMF. (b) The relation between $\ln(B_{g0})$ and $\ln(r_0)$ was transformed back to the one between B_{g0} and r_0 (plus signs) in order to compare the relation between B_{d0} and r_0 (diamonds). (c and d) Drawn in the same format as Figures 2a and 2b, respectively, except for northward IMF. The fitted line was overlaid on the data points in all panels.

with 95% confidence and 223 degrees of freedom is 3.88. The calculated F from the data is 248, which is much larger than the critical F. Thus, the derived relation between the two variables is not from the scattering of the data. Here we note that the F test relates to two variables. One relates fitted Y values to the average observed Y value. Its degree of freedom is one. The other relates fitted Y values to observed Y values. Its degree of freedom is the number of data points minus 2.

[12] The corresponding B_{d0} with respect to B_{g0} at the same position is also calculated under a consideration of the secular variations of the Earth's dipole tilt angle and the position of a magnetopause crossing. Each of the variables B_{g0} (pluses) and B_{d0} (diamonds) is individually plotted against r_0 for comparisons, as shown in Figure 2b. The derived power law exponent for B_{g0} versus r_0 is −1.68, in contrast to the expected −3 for the purely dipolar magnetic field.

[13] The same fitting procedure is applied to the magnetopause crossings for northward IMF (see Figures 2c and 2d). We find that $D = -2.42 \pm 0.08$ and $\ln(C) = 9.86 \pm 0.20$, with C being equal to 19080 ± 28 nT. The calculated F is 876, which is much larger than the critical F (3.87) tabulated with 95% confidence and 387 degrees of freedom. With the calculated C and D, (2) can be rewritten as

$$B_{g0} = 19080 r_0^{-2.42}. \quad (5)$$

[14] Figure 3a shows that the ratio f and r_0 have a linear relation, which can be fitted using the least squares method to a straight line, as follows:

$$f = G + H r_0, \quad (6)$$

where G and H are the parameters of the function. In the fit, the calculated F is 153, which is much larger than the critical F (3.88) tabulated with 95% confidence and 223 degrees of freedom. Therefore, the fit is statistically significant. The parameters G and H are estimated to be -0.80 ± 0.27 and 0.29 ± 0.02, respectively, and equation (6) can be rewritten as

$$f = -0.80 + 0.29 r_0. \quad (7)$$

Figure 3c shows the relation between the ratio f and the subsolar standoff distance r_0 for northward IMF. The parameters G and H are found to be 1.32 ± 0.21 and 0.10 ± 0.02, respectively. The calculated F (35.3) is larger than the critical F (3.87). It indicates that the derived relation is statistically significant. Equation (6) can be rewritten as

$$f = 1.32 + 0.10 r_0. \quad (8)$$

Figures 3b and 3d are a comparison between the difference $d = B_{g0} - B_{d0}$ and the subsolar standoff distance r_0 for both southward and northward IMF. The difference d indicates how much the magnetic field is increased by compression and/or magnetic erosion. The curves shown in Figures 3b and 3d represent the relation between r_0 and the expected difference predicted by theory $(2.44 - 1)30060 r_0^{-3}$. The spread of data points for southward IMF is larger than that for northward IMF, especially for $r_0 \leq 11\ R_E$, implying that the physical processes that control r_0 for southward IMF are more complicated than those for northward IMF. Compression and magnetic erosion interplay during southward IMF, while the

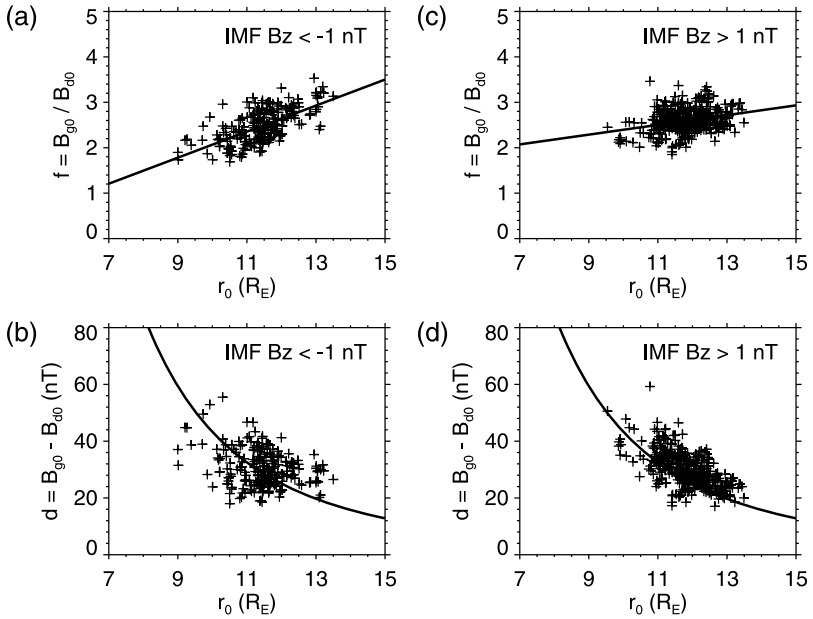

Figure 3. A ratio (f) of the compressed magnetic field just inside the subsolar magnetopause B_{g0} to the dipolar magnetic field B_{d0} and the difference between B_{g0} and B_{d0} in terms of the subsolar standoff distance r_0. (a) A linear least squares fitting of the ratio f to r_0 for southward IMF was performed. (b) The difference d was plotted against r_0. (c and d) Drawn in the same format as Figures 3a and 3b, respectively, except for northward IMF. The fitted line was overlaid on the data points in Figures 3a and 3c. The curves shown in Figures 3b and 3d represent the relation between r_0 and the expected difference predicted by theory $(2.44 - 1)30060r_0^{-3}$.

compression is the dominant effect in the compressed magnetic field during northward IMF.

4. Discussion and Conclusions

[15] Our division of events into northward and southward IMF is based on IMF $B_z > 1$ and $B_z < -1$ nT. However, this choice can still include events for small cone angles, the orientation of the IMF is aligned in less 30° with respect to the Sun-Earth line. As we know, the reconnection at the magnetopause is sensitive to the sign of IMF B_z for large and intermediate cone angles, but the sensitivity is less for small cone angles. To evaluate how the occurrence of the events for small cone angles affects the statistics, we recalculated the parameter D without including such events (16% of the total). The new D is -1.68 ± 0.12 for southward IMF, and is -2.43 ± 0.09 for northward IMF, which is almost the same as the value for the first calculation.

[16] Although B_{g0} can be affected by many factors, equation (2) appears to be a good functional form to model B_{g0}, as shown in Figures 2b and 2d. The fitting results show that the value of C in (2) determined for northward IMF is quite different from that determined for southward IMF. One may think that C should be ~30060 nT (the IGRF model value at 1 R_E) if the magnetopause moved to the Earth's surface. Here we emphasize that B_{g0} is the compressed magnetic field just inside the subsolar magnetopause, not the magnetic field at any place in the magnetosphere for a particular subsolar standoff distance r_0. If the magnetopause moved to the Earth's surface, B_{g0} would become more than double of the IGRF model value at 1 R_E. However, such a small standoff distance unlikely occurs. The smallest standoff distance ever documented is 5.2 R_E [*Hoffman et al.*, 1975]. Since the r_0 range for the data points used in this study is from 9 to 14 R_E, equations (4) and (5) are valid only at this range.

[17] Equations (4) and (5) are the first such empirical functions reported in the literature. The two equations not only can serve as a boundary condition in the global modeling of the magnetosphere [e.g., *Tsyganenko and Sitnov*, 2005], but also can advance our understandings of pressure balance between shocked solar wind and the Earth's magnetosphere or another planet's magnetosphere [*Huddleston et al.*, 1998; *Arridge et al.*, 2006].

[18] According to (7) and (8), if the subsolar distance r_0 is small, then so is the ratio f. Southward IMF increases the flaring of the magnetopause by magnetic reconnection [*Aubry et al.*, 1970; *Russell and McPherron*, 1973]. As a result, the shape of the magnetopause becomes more blunt when r_0 is smaller. From previous theoretical studies, the ratio f for the planar magnetosphere is 2 and that for the self-consistent magnetosphere is 2.44 [*Schield*, 1969]. Thus, the blunter shape is the magnetopause, the smaller is the ratio f. The same fitting procedure is applied to the magnetopause crossings for northward IMF. We find that the ratio f also depends upon r_0 for northward IMF, but the slope is smaller. Our results indicate that the ratio f should not be assumed to be independent of r_0 in the modeling of the solar wind–magnetosphere interaction.

[19] Figure 3 shows that the ratio f can be less than 2 or greater than 3. From a theoretical view, $f < 2$ may imply a globally concave magnetopause, namely, beyond the planar magnetopause. However, this configuration unlikely occurs. The cases for $f < 2$ are likely referred to "locally" indented magnetopause [e.g., *Shue et al.*, 2009]. In our results, the

majority of the cases for $f > 3$ are found at large r_0, an indicator of small dynamic pressure in the solar wind. For these cases, the outer magnetosphere has a lower magnetic field. As a result, the magnetopause becomes more sensitive to variations of the solar wind and the state of the magnetosphere [*Suvorova et al.*, 2010]. Some unusual responses of the magnetopause to the orientation of the IMF may easily occur, for example, the magnetopause becomes less blunt for southward IMF than for northward IMF. Another possibility for the unusual response is that the magnetopause is just convex locally because of the transient motion of the magnetopause for southward IMF.

[20] Our results show that the magnetic field just inside the magnetopause B_{g0} is not proportional to r_0^{-3}, suggesting that the size of the magnetosphere does not change as the solar wind dynamic pressure to the −1/6 exponent under an assumption of constant k. As we know, B_{g0} can change with Chapman Ferraro Currents, tail currents, and ring currents. The combination of these currents may affect its proportionality. If the k is not a constant, the exponent might not be −1/6. On the other hand, *Kuznetsov and Suvorova* [1998] reported that the value of the exponent depends upon the location of the magnetopause. The smallest value is found at the subsolar region. Our exponent values for northward and southward IMF determined at the subsolar region are smaller than −1/6, which is consistent with the previous study.

[21] In conclusion, the compressed magnetic field just inside the subsolar magnetopause varies with the subsolar standoff distance in a power law with an exponent −1.68 for southward IMF, and −2.42 for northward IMF, in contrast to the expected −3 for the purely dipolar field. It indicates that the ratio of the compressed magnetic field just inside the subsolar magnetopause to the purely dipolar magnetic field determined at the same location depends upon the subsolar standoff distance.

[22] **Acknowledgments.** This work was supported in part by National Science Council grants NSC-96-2111-M-008-008 and NSC-99-2111-M-008-005 to National Central University and in part by the Ministry of Education under the Aim for Top University Program at NCU. The solar wind data were provided by J. King through the OMNI Web page at http://omniweb.gsfc.nasa.gov/. We acknowledge NASA contract NAS5-02099.

[23] Philippa Browning thanks Nick Omidi and another reviewer for their assistance in evaluating this paper.

References

Angelopoulos, V. (2008), The THEMIS mission, *Space Sci. Rev.*, *141*(1–4), 5–34, doi:10.1007/s11214-008-9336-1.

Arridge, C. S., N. Achilleos, M. K. Dougherty, K. K. Khurana, and C. T. Russell (2006), Modeling the size and shape of Saturn's magnetopause with variable dynamic pressure, *J. Geophys. Res.*, *111*, A11227, doi:10.1029/2005JA011574.

Aubry, M. P., C. T. Russell, and M. G. Kivelson (1970), Inward motion of the magnetopause before a substorm, *J. Geophys. Res.*, *75*(34), 7018–7031.

Auster, H. U., et al. (2008), The THEMIS fluxgate magnetometer, *Space Sci. Rev.*, *141*(1–4), 235–264, doi:10.1007/s11214-008-9365-9.

Bevington, P. R., and D. K. Robinson (2003), *Data Reduction and Error Analysis for the Physical Sciences*, McGraw-Hill, New York.

Choe, J. Y., and D. B. Beard (1974), The compressed geomagnetic field as a function of dipole tilt, *Planet. Space Sci.*, *22*(4), 595–608.

Ferraro, V. C. A. (1960), An approximate method of estimating the size and shape of the stationary hollow carved out in a neutral ionized stream of corpuscles impinging on the geomagnetic field, *J. Geophys. Res.*, *65*(12), 3951–3953.

Glassmeier, K.-H., et al. (2008), Magnetospheric quasi-static response to the dynamic magnetosheath: A THEMIS case study, *Geophys. Res. Lett.*, *35*, L17S01, doi:10.1029/2008GL033469.

Hoffman, R. A., L. Cahill Jr., R. Anderson, N. Maynard, P. Smith, T. Fritz, D. Williams, A. Konradi, and D. Gurnett (1975), Explorer 45 (S^3-A) observations of the magnetosphere and magnetopause during the August 4–6, 1972, magnetic storm period, *J. Geophys. Res.*, *80*(31), 4287–4296.

Holzer, R. E., and J. A. Slavin (1978), Magnetic flux transfer associated with expansions and contractions of the dayside magnetosphere, *J. Geophys. Res.*, *83*(A8), 3831–3839.

Huddleston, D. E., C. Russell, M. Kivelson, K. Khurana, and L. Bennett (1998), Location and shape of the Jovian magnetopause and bow shock, *J. Geophys. Res.*, *103*(E9), 20,075–20,082.

King, J. H., and N. E. Papitashvili (2005), Solar wind spatial scales in and comparisons of hourly Wind and ACE plasma and magnetic field data, *J. Geophys. Res.*, *110*, A11206, doi:10.1029/2004JA010649.

Kivelson, M. G., and C. T. Russell (1995), *Introduction to Space Physics*, Cambridge Univ. Press, New York.

Kuznetsov, S. N., and A. V. Suvorova (1998), An empirical model of the magnetopause for broad ranges of solar wind pressure and B_z IMF, in *Polar Cap Boundary Phenomena*, edited by J. Moen et al., pp. 51–61, Kluwer Acad., Netherlands.

McFadden, J. P., et al. (2008), The THEMIS ESA plasma instrument and in-flight calibration, *Space Sci. Rev.*, *141*(1–4), 277–302, doi:10.1007/s11214-008-9440-2.

Mead, G. D. (1964), Deformation of the geomagnetic field by the solar wind, *J. Geophys. Res.*, *69*(7), 1181–1195.

Paschmann, G., I. Papamastorakis, W. Baumjohann, N. Sckopke, C. Carlson, B. Sonnerup, and H. Lühr (1986), The magnetopause for large magnetic shear: AMPTE/IRM observations, *J. Geophys. Res.*, *91*(A10), 11,099–11,115.

Petrinec, S. M., and C. T. Russell (1995), An examination of the effect of dipole tilt angle and cusp regions on the shape of the dayside magnetopause, *J. Geophys. Res.*, *100*(A6), 9559–9566.

Russell, C. T., and R. L. McPherron (1973), The magnetotail and substorms, *Space Sci. Rev.*, *15*(2–3), 205–266.

Schield, M. A. (1969), Pressure balance between solar wind and magnetosphere, *J. Geophys. Res.*, *74*(5), 1275–1286.

Shue, J.-H., J.-K. Chao, P. Song, J. P. McFadden, A. Suvorova, V. Angelopoulos, K. H. Glassmeier, and F. Plaschke (2009), Anomalous magnetosheath flows and distorted subsolar magnetopause for radial interplanetary magnetic fields, *Geophys. Res. Lett.*, *36*, L18112, doi:10.1029/2009GL039842.

Sibeck, D. G., R. E. Lopez, and E. C. Roelof (1991), Solar wind control of the magnetopause shape, location and motion, *J. Geophys. Res.*, *96*(A4), 5489–5495.

Spreiter, J. R., and B. R. Briggs (1962), Theoretical determination of the form of the boundary of the solar corpuscular stream produced by interaction with the magnetic dipole field of the Earth, *J. Geophys. Res.*, *67*(1), 37–51.

Suvorova, A. V., et al. (2010), Magnetopause expansions for quasi-radial interplanetary magnetic field: THEMIS and Geotail observations, *J. Geophys. Res.*, *115*, A10216, doi:10.1029/2010JA015404.

Tsyganenko, N. A., and M. I. Sitnov (2005), Modeling the dynamics of the inner magnetosphere during strong geomagnetic storms, *J. Geophys. Res.*, *110*, A03208, doi:10.1029/2004JA010798.

V. Angelopoulos and C. T. Russell, Institute of Geophysics and Planetary Physics, University of California, Los Angeles, CA 90095, USA. (vassilis@igpp.ucla.edu; ctrussel@igpp.ucla.edu)

Y.-S. Chen, W.-C. Hsieh, B. S. Lee, M. Nowada, and J.-H. Shue, Institute of Space Science, National Central University, Jhongli 32001, Taiwan. (hishyuan@gmail.com; simon@jupiter.ss.ncu.edu.tw; beson@jupiter.ss.ncu.edu.tw; nowada@jupiter.ss.ncu.edu.tw; jhshue@jupiter.ss.ncu.edu.tw)

K. H. Glassmeier, Institute of Geophysics and Extraterrestrial Physics, Technical University Braunschweig, D-38106 Braunschweig, Germany. (kh.glassmeier@tu-bs.de)

D. Larson and J. P. McFadden, Space Sciences Laboratory, University of California, Berkeley, CA 94720, USA. (davin@berkeley.edu; mcfadden@berkeley.edu)

P. Song, Center for Atmospheric Research, University of Massachusetts Lowell, Lowell, MA 01854, USA. (paul_song@uml.edu)